mathematics

Article

A Quasi-3D Higher-Order Theory for Bending of FG Nanoplates Embedded in an Elastic Medium in a Thermal Environment

Ashraf M. Zenkour [1,*], Mashhour A. Alazwari [2] and Ahmed F. Radwan [3]

1 Department of Mathematics, Faculty of Science, King Abdulaziz University, P.O. Box 80203, Jeddah 21589, Saudi Arabia
2 Mechanical Engineering Department, Faculty of Engineering, King Abdulaziz University, Jeddah 21589, Saudi Arabia; maalazwari@kau.edu.sa
3 Department of Mathematics and Statistics, High Institute of Management and Information Technology, Nile for Science and Technology Kafrelsheikh, Kafrelsheikh 33514, Egypt; a.f.radwan84@gmail.com
* Correspondence: zenkour@kau.edu.sa

Abstract: This paper presents the effects of temperature and the nonlocal coefficient on the bending response of functionally graded (FG) nanoplates embedded in an elastic foundation in a thermal environment. The effects of transverse normal strain, as well as transverse shear strains, are considered where the variation of the material properties of the FG nanoplate are considered only in thickness direction. Unlike other shear and deformations theories in which the number of unknown functions is five and more, the present work uses shear and deformations theory with only four unknown functions. The four-unknown normal and shear deformations model, associated with Eringen nonlocal elasticity theory, is used to derive the equations of equilibrium utilizing the principle of virtual displacements. The effects due to nonlocal coefficient, side-to-thickness ratio, aspect ratio, normal and shear deformations, thermal load and elastic foundation parameters, as well as the gradation in FG nanoplate bending, are investigated. In addition, for validation, the results obtained from the present work are compared to ones available in the literature.

Keywords: nonlocal theory; FG nanoplates; thermal load; four-unknown normal and shear deformations theory; elastic foundations

Citation: Zenkour, A.M.; Alazwari, M.A.; Radwan, A.F. A Quasi-3D Higher-Order Theory for Bending of FG Nanoplates Embedded in an Elastic Medium in a Thermal Environment. *Mathematics* **2022**, *10*, 234. https://doi.org/10.3390/math10020234

Academic Editor: Roman Starosta

Received: 16 December 2021
Accepted: 10 January 2022
Published: 13 January 2022

1. Introduction

Nanotechnology is the study of small objects and their applications and has many uses in scientific fields, such as physics, materials science, engineering, chemistry, and biology. For centuries, nanotechnology has been used even though modern nanoscience and nanotechnology are modern. Aifantis [1] discussed the interpretation of size effects using the strain gradient theory. Reddy [2] studied the bending, buckling, and vibration of beams utilizing nonlocal theories. Hashemi and Samaei [3] discussed the buckling of micro/nanoscale plates used the nonlocal elasticity theory. Zenkour and Sobhy [4] discussed the thermal buckling of nanoplates resting on Winkler–Pasternak foundations utilizing the nonlocal elasticity theory. The thermo-mechanical bending and free vibration behavior of single-layered graphene sheets lying on elastic foundations were studied by Sobhy [5].

Functionally graded materials (FGMs) consist of a mixture of metal and ceramic materials, which range from one material to the other following the law of volume fractions of the two materials through the thickness of the nanoplate [6–8]. Due to their distinct physical and thermal properties, the FGMs are preferable in many real-life applications. Maintaining the structural reliability of FGMs in a high thermal gradient environment is one of the advantages of using FGMs [9–13]. Consequently, many studies about the applications FG nanoplates/nanobeams can be found in the literature [14–19]. Zenkour et al. [20,21]

investigated the deflection and stresses of laminated plates resting on Winkler–Pasternak foundations in thermal and hygrothermal environments, respectively.

Due to the importance of designing foundations, various methods have been developed to study the response of beams and plates that are resting on elastic foundations such as Winkler's soil model [22] and Pasternak's model [23–28] and many other studies that are available in the literature [29–31]. However, most of the available shear and deformations theories used in the analysis involve five, six, and more unknown functions.

A refined four-unknown higher-order normal and shear deformations theory (RHT) for bending analysis of FG nanoplates embedded in elastic foundations is presented in this work where only four independent known functions are used. The equations of equilibrium are then analytically solved for bending and deflections of simply supported nanoplates to investigate the influence of the nonlocal parameter in which the material properties are influenced by the variation of temperature. The effects of foundation parameters, temperature, transverse normal deformation, plate aspect ratio, side-to-thickness ratio, nonlocal coefficient, and volume fraction on deflections and stresses are also investigated.

2. Geometrical Formulation

A rectangular $(a \times b)$ FG nanoplate is considered with thickness of h, as shown in Figure 1. The FG nanoplate is embedded in an elastic foundation and exposed to a distributed transverse load $q(x, y)$, as well as temperature $\mathcal{T}(x, y, z)$. According to two gradation models (Equations (1) and (2)), the material properties $\mathcal{P}_r$ such as the modulus of elasticity E and the thermal expansion coefficient α of the FG nanoplate with simply-supported edges in thermal environments, might be assumed:

$$\mathcal{P}_1(z) = \mathcal{P}_m + \mathcal{P}_{cm} V_\beta, \qquad V_\beta = \left(\frac{2z + h}{2h}\right)^\beta, \tag{1}$$

$$\mathcal{P}_2(z) = \mathcal{P}_m (\mathcal{P}_c / \mathcal{P}_m)^{V_\beta}, \tag{2}$$

where $\mathcal{P}_m$ is the property of the metal, $\mathcal{P}_{cm} = \mathcal{P}_c - \mathcal{P}_m$, $\mathcal{P}_c$ is the property of the ceramic and β is the FG parameter. In addition, Equations (1) and (2) implies that the upper surface of FG nanoplate $(z = +\frac{h}{2})$ is ceramic-rich, while the lower surface $(z = -\frac{h}{2})$ of FG nanoplate is metal-rich. The Poisson's ratio ν is generally assumed constant throughout the plate thickness and equal to 0.3. Based on the two gradation models, the variation of the modulus of elasticity E across the thickness of FG nanoplate for different values of the parameter β is shown in Figure 2.

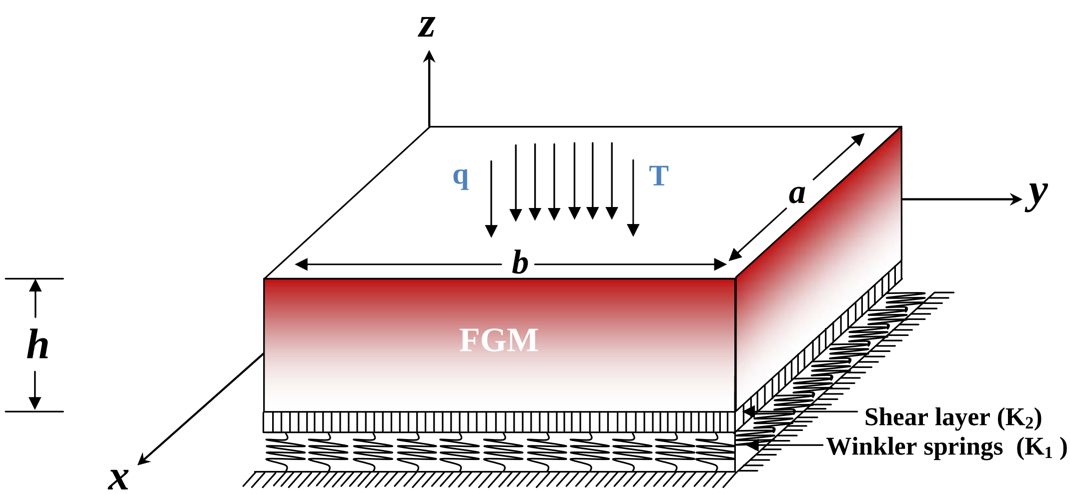

Figure 1. A rectangular FG nanoplates embedded in an elastic medium.

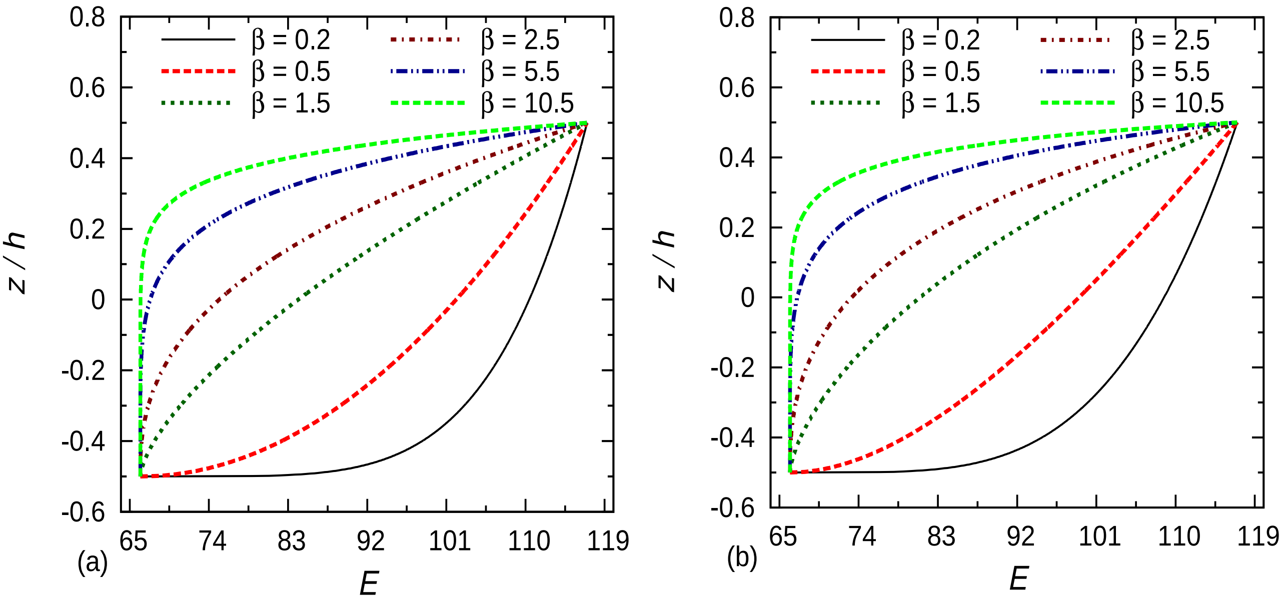

Figure 2. Variation of Young's modulus E through the thickness of the FG nanoplate for various values of the FG parameter β according to the two gradation models (**a**) model 1 and (**b**) model 2.

2.1. Nonlinear Thermal Conditions

For thermal-structural analysis, only linearly varying across the thickness temperature distribution $\mathcal{T}(x,y,z) = \mathcal{T}_1(x,y) + \frac{z}{h}\mathcal{T}_2(x,y)$ and nonlinear variation through the thickness temperature distribution $\mathcal{T}(x,y,z) = \frac{1}{h}\Psi(z)\mathcal{T}_3(x,y)$ and a combination of both are defined as [20,21]

$$\mathcal{T}(x,y,z) = \mathcal{T}_1(x,y) + \frac{z}{h}\mathcal{T}_2(x,y) + \frac{1}{h}\Psi(z)\mathcal{T}_3(x,y), \tag{3}$$

where $\Psi(z) = -\frac{z}{4}\left[1 - \frac{5}{3}\left(\frac{z}{h/2}\right)^2\right]$.

2.2. Displacements and Strains

The in-plane displacements, which are denoted as v_1 and v_2 and the transverse displacement v_3 in FG nanoplate are assumed according to a modified four-unknown normal and shear deformations theory (see in [32–38]):

$$\begin{aligned} v_1(x,y,z) &= u - z\partial_x w - \Psi(z)\partial_x\phi, \\ v_2(x,y,z) &= v - z\partial_y w - \Psi(z)\partial_y\phi, \\ v_3(x,y,z) &= w + \Big[1 + \xi\Phi(z)\Big]\phi. \end{aligned} \tag{4}$$

The function $\Psi(z)$ in the present theory should be odd function of z and $\Phi(z) = 1 - \Psi^{\backprime}$. The prime $(^{\backprime})$ represent differentiation with respect to z. The strain components compatible with the above displacement are given as

$$\begin{Bmatrix} \varepsilon_{xx} \\ \varepsilon_{yy} \\ \gamma_{xy} \end{Bmatrix} = \begin{Bmatrix} \varepsilon_x^0 \\ \varepsilon_y^0 \\ \gamma_{xy}^0 \end{Bmatrix} + z\begin{Bmatrix} \varepsilon_x^1 \\ \varepsilon_y^1 \\ \gamma_{xy}^1 \end{Bmatrix} + \Psi(z)\begin{Bmatrix} \varepsilon_x^2 \\ \varepsilon_y^2 \\ \gamma_{xy}^2 \end{Bmatrix}, \tag{5}$$
$$\gamma_{iz} = (1+\xi)\Phi(z)\gamma_{iz}^0, \qquad \varepsilon_{zz} = -\xi\Psi^{\backprime\backprime}\varepsilon_z^0, \quad (i = x, y),$$

where

$$\begin{aligned}
&\varepsilon_x^0 = \partial_x u, && \varepsilon_y^0 = \partial_y v, && \gamma_{xy}^0 = \partial_x v + \partial_y u,\\
&\varepsilon_x^1 = -\partial_{xx}^2 w, && \varepsilon_y^1 = -\partial_{yy}^2 w, && \gamma_{xy}^1 = -2\partial_{xy}^2 w,\\
&\varepsilon_x^2 = -\partial_{xx}^2 \phi, && \varepsilon_y^2 = -\partial_{yy}^2 \phi, && \gamma_{xy}^2 = -2\partial_{xy}^2 \phi,\\
&\gamma_{iz}^0 = \partial_i \phi, && \varepsilon_z^0 = \phi, && (i = x, y).
\end{aligned} \tag{6}$$

2.3. Constitutive Equations

For Eringen nonlocal elasticity theory [39–42], the nonlocal constitutive relations of an FG nanoplate in thermal environment are given as

$$\begin{aligned}
\left(1-\mu^2\nabla^2\right)\begin{Bmatrix}\sigma_{xx}\\ \sigma_{yy}\\ \sigma_{zz}\end{Bmatrix} &= \begin{bmatrix}c_{11} & c_{12} & c_{13}\\ c_{12} & c_{22} & c_{23}\\ c_{13} & c_{23} & c_{33}\end{bmatrix}\begin{Bmatrix}\varepsilon_{xx}-\alpha(z)\mathcal{T}\\ \varepsilon_{yy}-\alpha(z)\mathcal{T}\\ \varepsilon_{zz}-\alpha(z)\mathcal{T}\end{Bmatrix},\\
\left(1-\mu^2\nabla^2\right)\begin{Bmatrix}\sigma_{yz}\\ \sigma_{xz}\\ \sigma_{xy}\end{Bmatrix} &= \begin{bmatrix}c_{44} & 0 & 0\\ 0 & c_{55} & 0\\ 0 & 0 & c_{66}\end{bmatrix}\begin{Bmatrix}\gamma_{yz}\\ \gamma_{xz}\\ \gamma_{xy}\end{Bmatrix},
\end{aligned} \tag{7}$$

in which $\Re = 1 - \mu^2\nabla^2$ is the nonlocal operator and $\mu = e_0\ell$ is the small scale effect in nanostructures (i.e, the nonlocal coefficient), where e_0 is a constant and ℓ is an internal characteristic length. The constitutive constants c_{ij} may be expressed as

$$\begin{aligned}
c_{11}(z) = c_{22}(z) = c_{33}(z) &= \frac{(1-\nu)E(z)}{(1-2\nu)(1+\nu)},\\
c_{12}(z) = c_{13}(z) = c_{23}(z) &= \frac{\nu E(z)}{(1-2\nu)(1+\nu)},\\
c_{jj}(z) = G(z) = \frac{E(z)}{2+2\nu}, &\qquad (j = 4,5,6).
\end{aligned} \tag{8}$$

2.4. Governing Equations

In this section, we will use the principle of virtual displacements to get the equilibrium equations, that is,

$$\int_{-h/2}^{h/2}\int_{\Omega}\left[\sigma_{xx}\delta\varepsilon_{xx} + \sigma_{yy}\delta\varepsilon_{yy} + \sigma_{zz}\delta\varepsilon_{zz} + \sigma_{xy}\delta\gamma_{xy} + \sigma_{yz}\delta\gamma_{yz} + \sigma_{xz}\delta\gamma_{xz}\right]\mathrm{d}\Omega\mathrm{d}z + \int_{\Omega} V\mathrm{d}\Omega = 0, \tag{9}$$

where $V = (\Gamma - q)\delta v_3$ and $\Gamma = K_1 v_3 - K_2\left(\partial_{xx}^2 + \partial_{yy}^2\right)v_3$ is the virtual work done by elastic foundations and K_1 and K_2 are the Winkler-type and Pasternak-type foundations, respectively. Substitute Equations (5)–(7) into Equation (9) and integrate Equation (9) over the thickness of FG nanoplate:

$$\begin{aligned}
&\int_{\Omega}\Big[\mathcal{N}_x\delta\varepsilon_x^0 + \mathcal{N}_y\delta\varepsilon_y^0 + \mathcal{N}_z\delta\varepsilon_z^0 + \mathcal{N}_{xy}\delta\gamma_{xy}^0 + \mathcal{M}_x\delta\varepsilon_x^1 + \mathcal{M}_y\delta\varepsilon_y^1 + \mathcal{M}_{xy}\delta\gamma_{xy}^1 +\\
&\qquad \mathcal{S}_x\delta\varepsilon_x^2 + \mathcal{S}_y\delta\varepsilon_y^2 + \mathcal{S}_{xy}\delta\gamma_{xy}^2 + \mathcal{Q}_{xz}\delta\varepsilon_{xz}^0 + \mathcal{Q}_{yz}\delta\varepsilon_{yz}^0 + V\Big]\mathrm{d}\Omega = 0,
\end{aligned} \tag{10}$$

The stress resultants $\mathcal{N}$, $\mathcal{M}$, $\mathcal{S}$, and $\mathcal{Q}$ can be expressed as

$$\left(1-\mu^2\nabla^2\right)\begin{Bmatrix}\mathcal{N}_x\\ \mathcal{N}_y\\ \mathcal{M}_x\\ \mathcal{M}_y\\ \mathcal{S}_x\\ \mathcal{S}_y\\ \mathcal{S}_z\end{Bmatrix}=\begin{bmatrix}\mathcal{D}_{11} & \mathcal{D}_{12} & \mathcal{D}_{13} & \mathcal{D}_{14} & \mathcal{D}_{15} & \mathcal{D}_{16} & \mathcal{D}_{17}\\ & \mathcal{D}_{22} & \mathcal{D}_{23} & \mathcal{D}_{24} & \mathcal{D}_{25} & \mathcal{D}_{26} & \mathcal{D}_{27}\\ & & \mathcal{D}_{33} & \mathcal{D}_{34} & \mathcal{D}_{35} & \mathcal{D}_{36} & \mathcal{D}_{37}\\ & & & \mathcal{D}_{44} & \mathcal{D}_{45} & \mathcal{D}_{46} & \mathcal{D}_{47}\\ & & & & \mathcal{D}_{55} & \mathcal{D}_{56} & \mathcal{D}_{57}\\ & & & & & \mathcal{D}_{66} & \mathcal{D}_{67}\\ \text{symm.} & & & & & & \mathcal{D}_{77}\end{bmatrix}\begin{Bmatrix}\varepsilon_x^0\\ \varepsilon_y^0\\ \varepsilon_x^1\\ \varepsilon_y^1\\ \varepsilon_x^2\\ \varepsilon_y^2\\ \varepsilon_z^0\end{Bmatrix}-\begin{Bmatrix}\mathcal{N}_x^{\mathcal{T}}\\ \mathcal{N}_y^{\mathcal{T}}\\ \mathcal{M}_x^{\mathcal{T}}\\ \mathcal{M}_y^{\mathcal{T}}\\ \mathcal{S}_x^{\mathcal{T}}\\ \mathcal{S}_y^{\mathcal{T}}\\ \mathcal{N}_z^{\mathcal{T}}\end{Bmatrix},$$

$$\left(1-\mu^2\nabla^2\right)\begin{Bmatrix}\mathcal{N}_{xy}\\ \mathcal{M}_{xy}\\ \mathcal{S}_{xy}\end{Bmatrix}=\begin{bmatrix}\mathcal{A}_{11} & \mathcal{A}_{12} & \mathcal{A}_{13}\\ & \mathcal{A}_{22} & \mathcal{A}_{23}\\ \text{symm.} & & \mathcal{A}_{33}\end{bmatrix}\begin{Bmatrix}\gamma_{xy}^0\\ \gamma_{xy}^1\\ \gamma_{xy}^2\end{Bmatrix},$$

$$\left(1-\mu^2\nabla^2\right)(\mathcal{Q}_{xz},\mathcal{Q}_{yz})=(\mathcal{A}_{44}\gamma_{xz}^0,\mathcal{A}_{55}\gamma_{yz}^0). \tag{11}$$

The elements $\mathcal{D}_{ij}$ and $\mathcal{A}_{ij}$ appeared in Equation (11) are given in Appendix A. The thermal stress and moment resultants $\mathcal{N}_i^{\mathcal{T}}$, $\mathcal{M}_i^{\mathcal{T}}$ and $\mathcal{S}_i^{\mathcal{T}}$ are defined by

$$\begin{aligned}\{\mathcal{N}_x^{\mathcal{T}},\mathcal{M}_x^{\mathcal{T}},\mathcal{S}_x^{\mathcal{T}}\}&=\int_{-h/2}^{h/2}(c_{11}+c_{12}+c_{13})(1,z,\Psi(z))\alpha\mathcal{T}\mathrm{d}z,\\ \{\mathcal{N}_y^{\mathcal{T}},\mathcal{M}_y^{\mathcal{T}},\mathcal{S}_y^{\mathcal{T}}\}&=\int_{-h/2}^{h/2}(c_{12}+c_{22}+c_{23})(1,z,\Psi(z))\alpha\mathcal{T}\mathrm{d}z,\\ \mathcal{N}_z^{\mathcal{T}}&=-\xi\int_{-h/2}^{h/2}\Psi''(z)(c_{13}+c_{23}+c_{33})\alpha\mathcal{T}\mathrm{d}z.\end{aligned} \tag{12}$$

According to Equation (10) the equilibrium equations can be written as

$$\begin{aligned}\delta u:&\quad \frac{\partial\mathcal{N}_x}{\partial x}+\frac{\partial\mathcal{N}_{xy}}{\partial y}=0,\\ \delta v:&\quad \frac{\partial\mathcal{N}_{xy}}{\partial x}+\frac{\partial\mathcal{N}_y}{\partial y}=0,\\ \delta w:&\quad \frac{\partial^2\mathcal{M}_x}{\partial x^2}+2\frac{\partial^2\mathcal{M}_{xy}}{\partial xy}+\frac{\partial^2\mathcal{M}_y}{\partial y^2}+\left(1-\mu^2\nabla^2\right)(q-\Gamma)=0,\\ \delta\phi:&\quad \frac{\partial^2\mathcal{S}_x}{\partial x^2}+2\frac{\partial^2\mathcal{S}_{xy}}{\partial xy}+\frac{\partial^2\mathcal{S}_y}{\partial y^2}+\frac{\partial\mathcal{Q}_{yz}}{\partial y}+\frac{\partial\mathcal{Q}_{xz}}{\partial x}-\mathcal{N}_z+\left(1-\mu^2\nabla^2\right)(q-\Gamma)=0.\end{aligned} \tag{13}$$

Substituting Equation (11) into Equation (13) yields a system of simultaneous algebraic equations:

$$[\mathcal{K}]\{\delta\}=\{f\}, \tag{14}$$

where the elements $\mathcal{K}_{ij}=\mathcal{K}_{ji}$ are the differential operators and given in Appendix B. The vector $\{f\}=\{f_1,f_2,f_3,f_4\}^{\mathrm{t}}$, while $\{\delta\}=\{u,v,w,\psi\}^{\mathrm{t}}$. The components of the force vector $\{f\}$ are given as

$$\begin{aligned}f_1&=\partial_x\mathcal{N}_x^{\mathcal{T}}, & f_3&=\partial_{xx}^2\mathcal{M}_x^{\mathcal{T}}+\partial_{yy}^2\mathcal{M}_y^{\mathcal{T}}-\left(1-\mu^2\nabla^2\right)q,\\ f_2&=\partial_y\mathcal{N}_y^{\mathcal{T}}, & f_4&=\partial_{xx}^2\mathcal{S}_x^{\mathcal{T}}+\partial_{yy}^2\mathcal{S}_y^{\mathcal{T}}+\mathcal{N}_z^{\mathcal{T}}-\left(1-\mu^2\nabla^2\right)q.\end{aligned} \tag{15}$$

3. Closed-Form Solution

The external force and the thermal loads proposed by Navier are used to solve the operator Equation (14), which are given as

$$q(x,y) = \sum_{m,n=1,3,5,\ldots}^{\infty} q_{mn} \sin(\lambda_m x) \sin(\gamma_n y), \qquad q_{mn} = \frac{16 q_0}{mn\pi^2},$$
$$\mathcal{T}_s = t_s \sin(\lambda_m x) \sin(\gamma_n y), \qquad s = 1,2,3, \tag{16}$$

and for the simply-supported boundary conditions at the side edges for the FG nanoplate are imposed as

$$\begin{aligned} v = w = \partial_y \psi = \mathcal{N}_x = \mathcal{M}_x = \mathcal{S}_x = 0 \qquad \text{at} \quad x = 0, a, \\ u = w = \partial_x \psi = \mathcal{N}_y = \mathcal{M}_y = \mathcal{S}_y = 0 \qquad \text{at} \quad y = 0, b. \end{aligned} \tag{17}$$

and $\lambda_m = \frac{m\pi}{a}$, $\gamma_n = \frac{n\pi}{b}$, t_s are constants. At $m = n = 1$ then the sinusoidal load is considered and $q_{11} = q_0$. According to the given boundary conditions, the Navier solution for u, v, w, and ψ is assumed as

$$\begin{Bmatrix} u \\ v \\ w \\ \psi \end{Bmatrix} = \begin{Bmatrix} U^1_{mn} \cos(\lambda_m x) \sin(\gamma_n y) \\ U^2_{mn} \sin(\lambda_m x) \cos(\gamma_n y) \\ U^3_{mn} \sin(\lambda_m x) \sin(\gamma_n y) \\ U^4_{mn} \sin(\lambda_m x) \sin(\gamma_n y) \end{Bmatrix}, \tag{18}$$

where $U^1_{mn}, U^2_{mn}, U^3_{mn}$, and U^4_{mn} are arbitrary parameters. Substituting Equation (18) into Equation (14) leads to a system of simultaneous algebraic equations, which can be expressed in a compact form as

$$[\mathcal{H}]\{\Delta\} = \{\mathcal{F}\}, \tag{19}$$

where $\{\Delta\}$ and $\{\mathcal{F}\}$ represent the columns:

$$\begin{aligned} \{\Delta\} &= \{U^1_{mn}, U^2_{mn}, U^3_{mn}, U^4_{mn}\}^{\mathrm{t}}, \\ \{\mathcal{F}\} &= \{\mathcal{F}_1, \mathcal{F}_2, \mathcal{F}_3, \mathcal{F}_4\}^{\mathrm{t}}, \end{aligned} \tag{20}$$

in which

$$\begin{aligned} \mathcal{F}_1 &= \lambda_m \sum_{j=1}^{3} \left[e^{\mathcal{T}}_{1j} t_j\right] \left[1 + \mu^2 \left(\lambda_m^2 + \gamma_n^2\right)\right], \\ \mathcal{F}_2 &= \gamma_n \sum_{j=1}^{3} \left[e^{\mathcal{T}}_{2j} t_j\right] \left[1 + \mu^2 \left(\lambda_m^2 + \gamma_n^2\right)\right], \\ \mathcal{F}_3 &= -\left\{ \sum_{j=1}^{3} \left[\lambda_m^2 \left(e^{\mathcal{T}}_{3j} t_j\right) + \gamma_n^2 \left(e^{\mathcal{T}}_{4j} t_j\right)\right] + q_0 \right\} \left[1 + \mu^2 \left(\lambda_m^2 + \gamma_n^2\right)\right], \\ \mathcal{F}_4 &= -\left\{ \sum_{j=1}^{3} \left[\lambda_m^2 \left(e^{\mathcal{T}}_{5j} t_j\right) + \gamma_n^2 \left(e^{\mathcal{T}}_{6j} t_j\right) - \left(e^{\mathcal{T}}_{7j} t_j\right)\right] + q_0 \right\} \left[1 + \mu^2 \left(\lambda_m^2 + \gamma_n^2\right)\right]. \end{aligned} \tag{21}$$

The elements $\mathcal{H}_{ij} = \mathcal{H}_{ji}$ of the coefficient matrix $[\mathcal{H}]$ and $e^{\mathcal{T}}_{ij}$ are given in Appendix C.

4. Numerical Results

The numerical results are calculated to verify the accuracy of the present theory in predicting the effects of the nonlocal coefficient on the bending response of the simply-supported FG nanoplates embedded in elastic foundations under thermal load. The upper surface $(z = +\frac{h}{2})$ of FG nanoplate is titanium, while the lower surface $(z = -\frac{h}{2})$ of FG nanoplate is Zirconia. In the case of mechanical bending, only the nanoplate is made from alumina (Al_2O_3) and aluminum (Al). Table 1 gives the material properties of the FG nanoplate. For verification purposes, the present outcomes are compared well to various plate theories, and a good agreement is observed. It is found that the best value of ξ that provides accurate and efficient results is $\xi = 2/15$. The following fixed data are

$q_0 = 100, \beta = 1.5, a = 10h, a = b, t_1 = 0, a = 10nm$ (unless otherwise stated). The following dimensionless deflection, stresses, and foundation parameters are applied as:

$$\bar{w} = \frac{10^2 D}{q_0 a^4} v_3\left(\frac{a}{2}, \frac{b}{2}, 0\right), \quad w^* = \frac{10h^3 E_c}{q_0 a^4} v_3\left(\frac{a}{2}, \frac{b}{2}, 0\right), \quad \kappa_1 = \frac{a^4}{D} K_1,$$
$$\sigma_1 = \frac{h}{q_0 a}\sigma_{xx}\left(\frac{a}{2}, \frac{b}{2}, \frac{z}{h}\right), \quad \sigma_2 = \frac{h}{q_0 a}\sigma_{yy}\left(\frac{a}{2}, \frac{b}{2}, \frac{z}{h}\right), \quad \kappa_2 = \frac{a^2}{D} K_2,$$
$$\sigma_4 = -\frac{h}{q_0 a}\sigma_{yz}\left(\frac{a}{2}, 0, 0\right), \quad \sigma_5 = -\frac{h}{q_0 a}\sigma_{xz}\left(0, \frac{b}{2}, 0\right),$$
$$\sigma_6 = \frac{h}{q_0 a}\sigma_{xy}\left(0, 0, -\frac{h}{2}\right), \quad \sigma_3 = -\frac{h}{q_0 a}\sigma_{zz}\left(\frac{a}{2}, \frac{b}{2}, \frac{z}{h}\right),$$

where $D = \frac{h^3 E}{12(1-\nu^2)}$. The deflection and stresses due to the thermal bending for FG nanoplates resting on Winkler–Pasternak foundations are presented. Results are reported in Tables 2–8 and Figures 3–9, where the results in Tables 2–4 and 7 are obtained by using the first gradation model given in Equation (1); however, the results in Tables 5, 6, and 8 and Figures 3–9 are obtained by using the second gradation model given in Equation (2).

Table 1. Material properties used in the FG nanoplate.

	Mechanical Bending		Thermal Bending	
Properties	**Aluminum**	**Alumina**	**Titanium**	**Zirconia**
E (GPa)	70	380	66.2	117
ν	0.3	0.3	1/3	1/3
α (10^{-6}/°C)	—	—	10.3	7.11

Table 2. Nondimensionalized deflection $w^*(0)$ of and the in-plane normal stress $\sigma_1(h/3)$ in FG square plates under sinusoidal loads.

		w^*			σ_1		
β	**Theory**	$a/h = 4$	**10**	**100**	$a/h = 4$	**10**	**100**
1	Ref. [43]	0.729	0.589	0.563	0.806	2.015	20.150
	Ref. [44]	0.717	0.588	0.563	0.622	1.506	14.969
	Ref. [45]	0.700	0.585	0.562	0.593	1.495	14.969
	Present	0.6929	0.5685	0.5462	0.5795	1.4647	14.549
4	Ref. [43]	1.113	0.874	0.829	0.642	1.605	16.049
	Ref. [44]	1.159	0.882	0.829	0.488	1.197	11.923
	Ref. [45]	1.118	0.875	0.829	0.440	1.178	11.932
	Present	1.0945	0.8411	0.7933	0.4204	1.1241	11.3919
10	Ref. [43]	1.318	0.997	0.936	0.480	1.199	11.990
	Ref. [44]	1.375	1.007	0.936	0.370	0.897	8.908
	Ref. [45]	1.349	0.875	0.829	0.323	1.178	11.932
	Present	1.3247	0.9786	0.9139	0.3089	0.8438	8.5898

Table 3. Comparison of non-dimensional deflection and stresses of FG square plate under sinusoidal distributed load ($a = 10h$).

β	Theory	w^*	σ_1	σ_2	σ_6	σ_4	σ_5
ceramic	Ref. [46]	0.2960	1.9955	1.3121	0.7065	0.2132	0.2462
	present	0.2936	2.0211	1.3240	0.6932	0.2428	0.2731
1	Ref. [46]	0.5889	3.0870	1.4894	0.6110	0.2622	0.2462
	present	0.5684	3.1022	1.4647	0.5618	0.2985	0.2731
2	Ref. [46]	0.7573	3.6094	1.3954	0.5441	0.2763	0.2265
	present	0.7224	3.6032	1.3509	0.4944	0.2758	0.2202
3	Ref. [46]	0.8377	3.8742	1.2748	0.5525	0.2715	0.2107
	present	0.7977	3.8407	1.2218	0.5028	0.2429	0.1837
4	Ref. [46]	0.8819	4.0693	1.1783	0.5667	0.2580	0.2029
	present	0.8411	4.0129	1.1241	0.5184	0.2149	0.1647
5	Ref. [46]	0.9118	4.2488	1.1029	0.5755	0.2429	0.2017
	present	0.8720	4.1760	1.0510	0.5292	0.1941	0.1569
6	Ref. [46]	0.9356	4.4244	1.0417	0.5803	0.2296	0.2041
	present	0.8974	4.3405	0.9934	0.5365	0.1797	0.1556
7	Ref. [46]	0.9562	4.5971	0.9903	0.5834	0.2194	0.2081
	present	0.9199	4.5062	0.9460	0.5419	0.1704	0.1575
8	Ref. [46]	0.9750	4.7661	0.9466	0.5856	0.2121	0.2124
	present	0.9407	4.6712	0.9062	0.5462	0.1648	0.1608
9	Ref. [46]	0.9925	4.9303	0.9092	0.5875	0.2072	0.2164
	present	0.9602	4.8334	0.8723	0.5501	0.1619	0.1648
10	Ref. [46]	1.0089	5.0890	0.8775	0.5894	0.2041	0.2198
	present	0.9786	4.9916	0.8438	0.5536	0.1609	0.1689
metal	Ref. [46]	1.6070	1.9955	1.3121	0.7065	0.2132	0.2462
	present	1.5938	2.0211	1.3240	0.6932	0.2428	0.2731

Table 4. Comparison of non-dimensional deflection $10\bar{w}$ of square plate subjected to uniformly distributed load.

		$a/h = 10$			$a/h = 200$		
κ_1	κ_2	**Ref.** [47]	**Ref.** [26]	**Present**	**Ref.** [47]	**Ref.** [26]	**Present**
1	5	3.3455	3.3455	3.16463	3.2200	3.2200	3.21954
	10	2.7505	2.7504	2.60969	2.6684	2.6684	2.66805
	15	2.3331	2.3331	2.21865	2.2763	2.2763	2.27599
	20	2.0244	2.0244	1.92843	1.9834	1.9834	1.98315
3^4	5	2.8422	2.8421	2.69617	2.7552	2.7552	2.75481
	10	2.3983	2.3983	2.28056	2.3390	2.3390	2.33863
	15	2.0730	2.0730	1.97479	2.0306	2.0306	2.03035
	20	1.8245	1.8244	1.74054	1.7932	1.7932	1.79296
5^4	5	1.3785	1.3785	1.32246	1.3688	1.3688	1.36864
	10	1.2615	1.2615	1.21104	1.2543	1.2543	1.25412
	15	1.1627	1.1627	1.11682	1.1572	1.1572	1.15710
	20	1.0782	1.0782	1.03612	1.0740	1.0740	1.07389

Table 5. Effects of the nonlocal coefficient, FG parameter and foundation parameters on the deflection 10 w^* of and in-plane normal stress σ_1 in the FG square nanoplate $(a/h = 10)$.

				(κ_1, κ_2) *			(κ_1, κ_2) **		
	β	**Theory**	ε_z	**(0,0)**	**(100,0)**	**(100,100)**	**(0,0)**	**(100,0)**	**(100,100)**
10 w^*	0	Ref. [48]	$= 0$	2.9603	2.3290	0.4470	5.2977	3.5671	0.4789
		present	$\neq 0$	2.9359	2.3183	0.4499	5.2539	3.5577	0.4825
	0.5	Ref. [48]	$= 0$	5.4971	3.6564	0.4805	9.8374	5.1752	0.4998
		present	$\neq 0$	5.3352	3.5937	0.4828	9.5477	5.1133	0.5029
	2.5	Ref. [48]	$= 0$	8.8382	4.8847	0.4969	15.8166	6.4599	0.5096
		present	$\neq 0$	8.4675	4.7865	0.4996	15.1532	6.3769	0.5129
	5.5	Ref. [48]	$= 0$	10.0219	5.2259	0.5003	17.9350	6.7874	0.5115
		present	$\neq 0$	9.7162	5.1633	0.5038	17.3878	6.7447	0.5156
	10.5	Ref. [48]	$= 0$	11.1361	5.5135	0.5028	19.9288	7.0545	0.5130
		present	$\neq 0$	10.9327	5.4889	0.5069	19.5648	7.0506	0.5175
σ_1	0	Ref. [48]	$= 0$	19.9550	15.6991	3.0133	35.7108	24.0455	3.2284
		present	$\neq 0$	20.2107	15.9589	3.0973	36.1685	24.4916	3.3219
	0.5	Ref. [48]	$= 0$	29.6544	19.7250	2.5922	53.0686	27.9183	2.6962
		present	$\neq 0$	29.7803	20.0596	2.6950	53.2939	28.5419	2.8071
	2.5	Ref. [48]	$= 0$	41.8345	23.1212	2.3522	74.8658	30.5774	2.4120
		present	$\neq 0$	41.3041	23.3484	2.4369	73.9165	31.1065	2.5021
	5.5	Ref. [48]	$= 0$	50.4378	26.3004	2.5177	90.2620	34.1591	2.5744
		present	$\neq 0$	49.5517	26.3324	2.5691	88.6762	34.3973	2.6293
	10.5	Ref. [48]	$= 0$	61.1311	30.2661	2.7599	109.3982	38.7253	2.8160
		present	$\neq 0$	60.3469	30.2976	2.7978	107.9948	38.9185	2.8563

The superscript * denotes $\mu = 0$ and ** denotes $\mu = 2$.

Table 6. Effects of the nonlocal coefficient and FG parameter on transverse shear stress σ_5 and in-plane tangential stress σ_6 in the FG square nanoplate for different values of the foundation parameters $(a/h = 10)$.

				(κ_1, κ_2) *			(κ_1, κ_2) **		
	β	**Theory**	ε_z	**(0,0)**	**(100,0)**	**(100,100)**	**(0,0)**	**(100,0)**	**(100,100)**
σ_5	0	Ref. [48]	$= 0$	2.4618	1.9368	0.3717	4.4056	2.9664	0.3983
		present	$\neq 0$	2.7311	2.1566	0.4185	4.8876	3.3096	0.4489
	0.5	Ref. [48]	$= 0$	2.4559	1.6336	0.2147	4.3950	2.3121	0.2233
		present	$\neq 0$	2.7183	1.8309	0.2459	4.8645	2.6052	0.2562
	2.5	Ref. [48]	$= 0$	2.1227	1.1732	0.1194	3.7988	1.5515	0.1224
		present	$\neq 0$	1.7774	1.0047	0.1049	3.1808	1.3386	0.1077
	5.5	Ref. [48]	$= 0$	2.1679	1.1304	0.1082	3.8796	1.4682	0.1107
		present	$\neq 0$	1.7118	0.9097	0.0888	3.0634	1.1883	0.0908
	10.5	Ref. [48]	$= 0$	2.3001	1.1388	0.1038	4.1162	1.4571	0.1060
		present	$\neq 0$	1.9363	0.9721	0.0898	3.4651	1.2487	0.0916
σ_6	0	Ref. [48]	$= 0$	10.7450	8.4534	1.6226	19.2289	12.9475	1.7383
		present	$\neq 0$	10.5389	8.3218	1.6151	18.8601	12.7712	1.7322
	0.5	Ref. [48]	$= 0$	4.4493	2.9595	0.3889	7.9624	4.1888	0.4045
		present	$\neq 0$	4.1639	2.8048	0.3768	7.4517	3.9908	0.3925
	2.5	Ref. [48]	$= 0$	7.5813	4.1900	0.4263	13.5671	5.5412	0.4371
		present	$\neq 0$	7.0295	3.9736	0.4147	12.5797	5.2939	0.4258
	5.5	Ref. [48]	$= 0$	8.1777	4.2642	0.4082	14.6345	5.5383	0.4173
		present	$\neq 0$	7.7237	4.1045	0.4005	13.8222	5.3616	0.4098
	10.5	Ref. [48]	$= 0$	8.5915	4.2537	0.3879	15.3751	5.4425	0.3957
		present	$\neq 0$	8.2471	4.1405	0.3824	14.7587	5.3186	0.3903

The superscript * denotes $\mu = 0$ and ** denotes $\mu = 2$.

Table 7. Effects of the FG parameter β and thermal loads on the transverse normal stress σ_3 and transverse shear stress σ_5 of a sinusoidal distributed loaded FG plate resting on elastic foundations ($a = 10h$).

					σ_3		σ_5	
β	t_2	t_3	κ_1	κ_2	$a = b$	$a = 3b$	$a = b$	$a = 3b$
1	10	0	10	0	0.48746	0.38594	0.60708	0.33318
			10	10	0.32324	0.34652	0.94541	0.40092
	50	0	10	0	1.87987	1.81455	4.18383	1.86379
			10	10	1.28029	1.63318	5.41912	2.17549
	50	50	10	0	1.87576	1.81042	4.16179	1.82721
			10	10	1.27622	1.62833	5.39699	2.14016
3	10	0	10	0	0.38912	0.29807	0.52052	0.30127
			10	10	0.23874	0.26176	0.82659	0.36535
	50	0	10	0	1.44371	1.38628	3.62410	1.68999
			10	10	0.90245	1.22039	4.72572	1.98281
	50	50	10	0	1.45633	1.39903	3.61608	1.66221
			10	10	0.91362	1.23191	4.72064	1.95719
5	10	0	10	0	0.30534	0.23133	0.50168	0.29444
			10	10	0.18281	0.20146	0.80330	0.35847
	50	0	10	0	1.12079	1.07195	3.50757	1.65380
			10	10	0.68188	0.93579	4.58793	1.94566
	50	50	10	0	1.11778	1.06916	3.50444	1.62887
			10	10	0.67731	0.93184	4.58865	1.92322
10	10	0	10	0	0.20486	0.15336	0.50286	0.29515
			10	10	0.11918	0.13195	0.81804	0.36261
	50	0	10	0	0.74464	0.70768	3.54313	1.66206
			10	10	0.43925	0.61024	4.66649	1.96915
	50	50	10	0	0.71976	0.68308	3.54437	1.63893
			10	10	0.41302	0.58472	4.67273	1.94892

Table 8. Effects of the nonlocal coefficient and thermal parameters on the deflection $\bar{w}$ of and transverse normal stress σ_3 in the FG square nanoplate embedded in an elastic medium ($\kappa_1 = \kappa_2 = 10$, $a/h = 10$, $\beta = 2$).

			μ				
	t_2	t_3	**0**	**0.5**	**1**	**1.5**	**2**
$\bar{w}$	10	10	1.21750	1.24068	1.30230	1.38399	2.54608
		50	2.15900	1.28133	1.34504	1.42952	1.51561
	20	10	2.11913	2.15908	2.26507	2.40491	3.35866
		50	2.15900	2.19973	2.30779	2.45043	2.59450
	50	10	4.82403	4.91429	5.15336	5.46765	5.78275
		50	4.86389	4.95494	5.19609	5.51317	5.83117
	100	10	9.33219	9.50629	9.96717	10.57220	11.17721
		50	9.37206	9.54695	10.00990	10.61773	11.22563
σ_3	10	10	0.13637	0.16288	0.24665	0.39753	0.62548
		50	0.05472	0.07783	0.15156	0.28608	0.49165
	20	10	0.45713	0.51432	0.69335	1.01145	1.48607
		50	0.37547	0.42928	0.59826	0.89999	1.35223
	50	10	1.41939	1.56865	2.03345	2.85321	4.06783
		50	1.33773	1.48360	1.93836	2.74175	3.93399
	100	10	3.02316	3.32587	4.26694	5.92280	8.37076
		50	2.94150	3.24082	4.17185	5.81135	8.23692

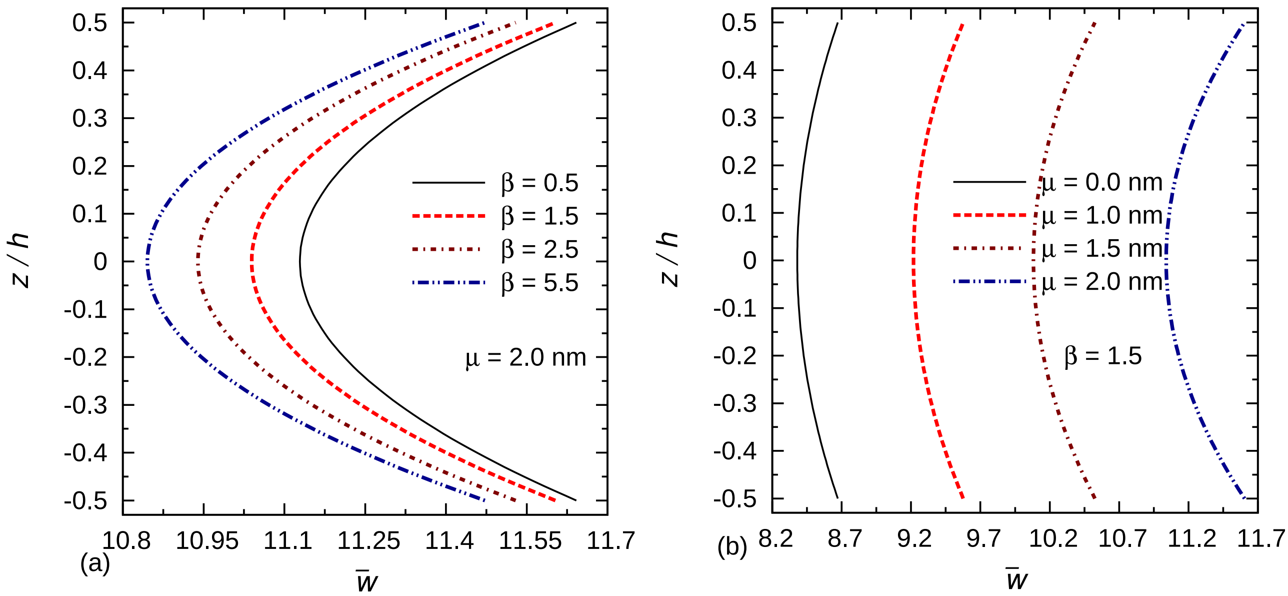

Figure 3. Effects of (**a**) FG parameter β and (**b**) nonlocal coefficient μ on the deflection $\bar{w}$ through-the-thickness of the FG square nanoplates embedded in an elastic medium ($a = 10h, t_2 = t_3 = 200$, $\kappa_1 = \kappa_2 = 10$).

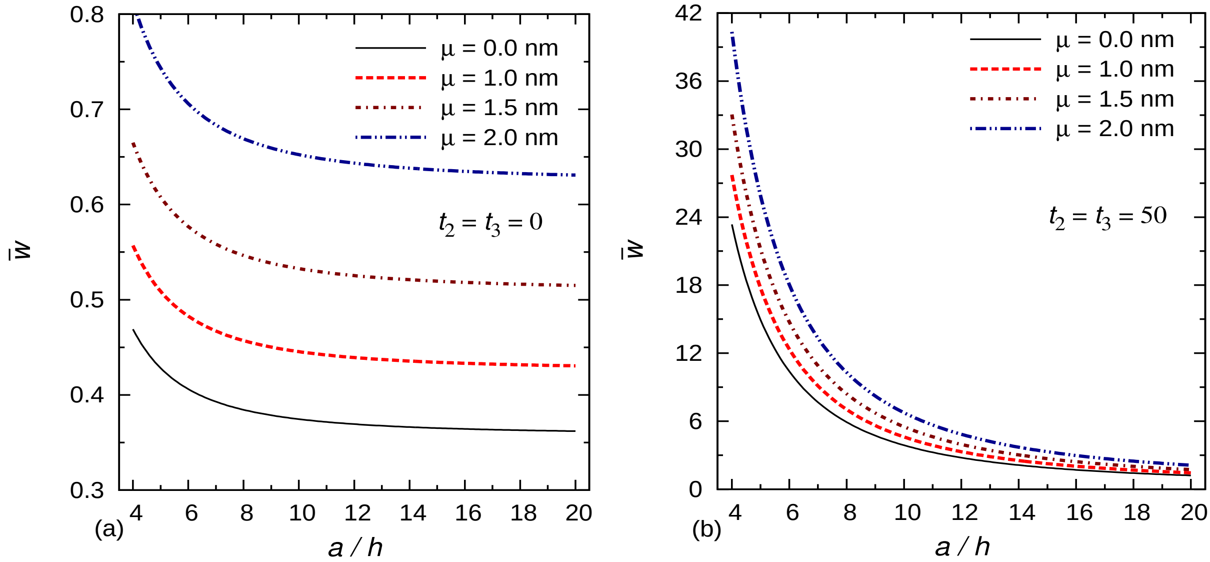

Figure 4. Effects of the nonlocal coefficient and thermal loads versus the side-to-thickness ratio a/h on the deflection $\bar{w}$ of the FG square nanoplates embedded in Winkler elastic medium (**a**) $t_2 = t_3 = 0$ and (**b**) $t_2 = t_3 = 50$ ($z/h = 0, \kappa_1 = 10, \kappa_2 = 0$).

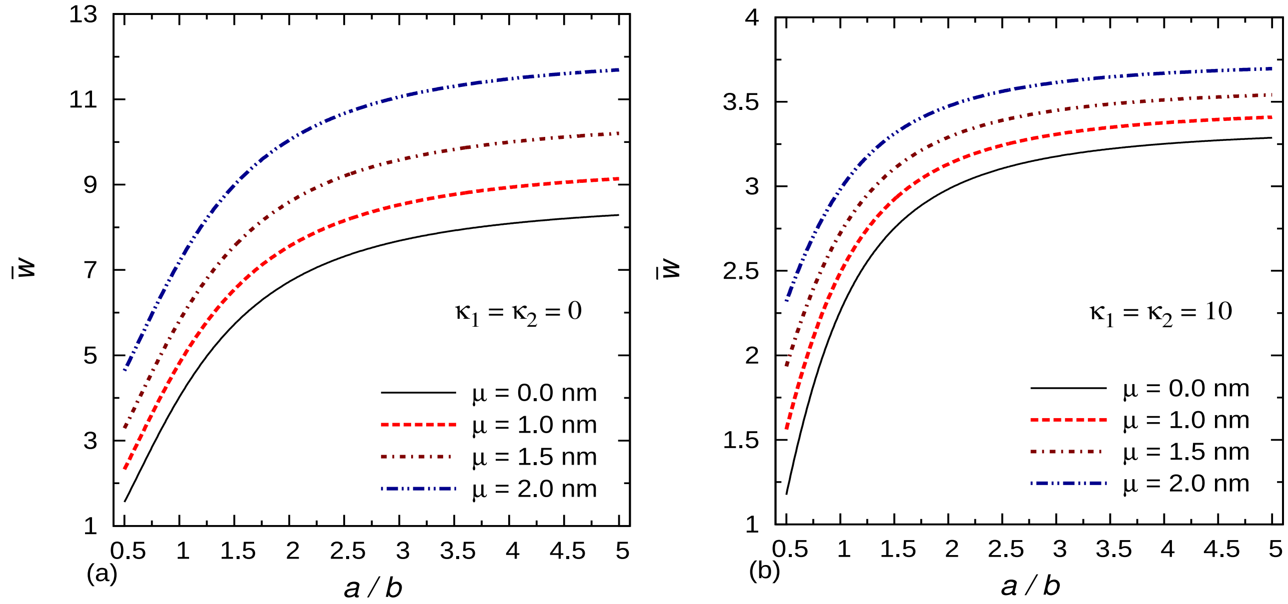

Figure 5. Effect of the nonlocal coefficient μ on the deflection $\bar{w}$ of the FG nanoplate versus aspect ratio a/b (**a**) $\kappa_1 = \kappa_2 = 0$ and (**b**) $\kappa_1 = \kappa_2 = 10$ $(z/h = 0, a/h = 10, t_2 = t_3 = 50)$.

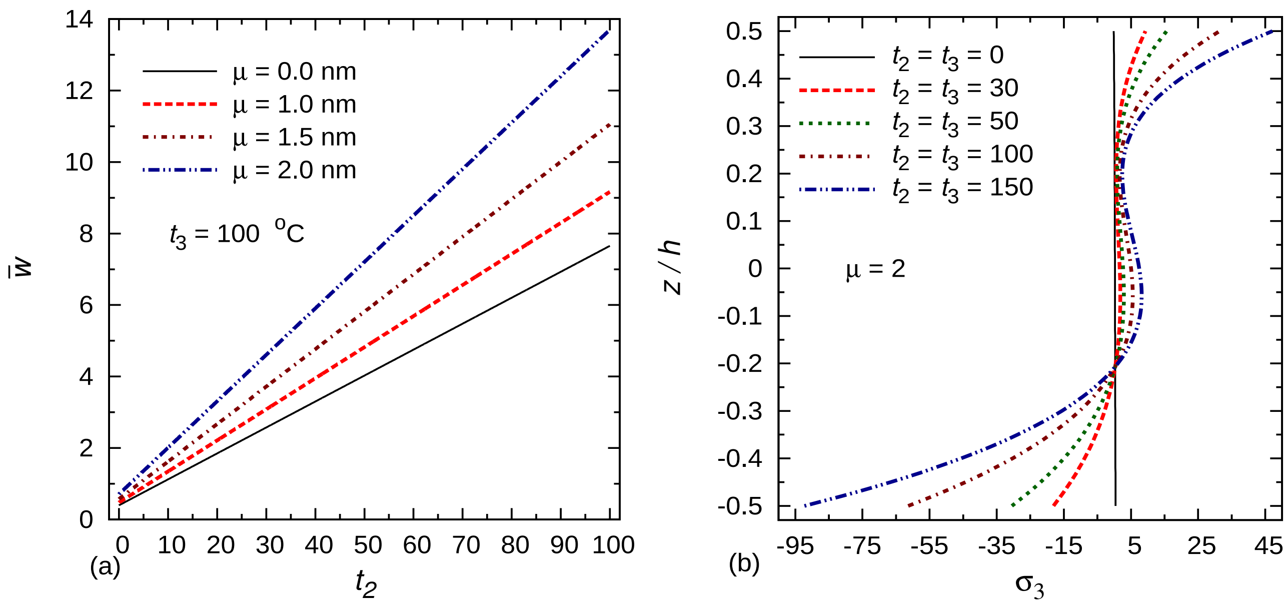

Figure 6. (**a**) Effect of the nonlocal coefficient μ on the deflection $\bar{w}$ $(z/h = 0)$ and (**b**) effect of the thermal loads t_2 and t_3 on the transverse normal stress σ_3 through the thickness in FG square nanoplates ($\kappa_1 = \kappa_2 = 0$, $a/h = 10$).

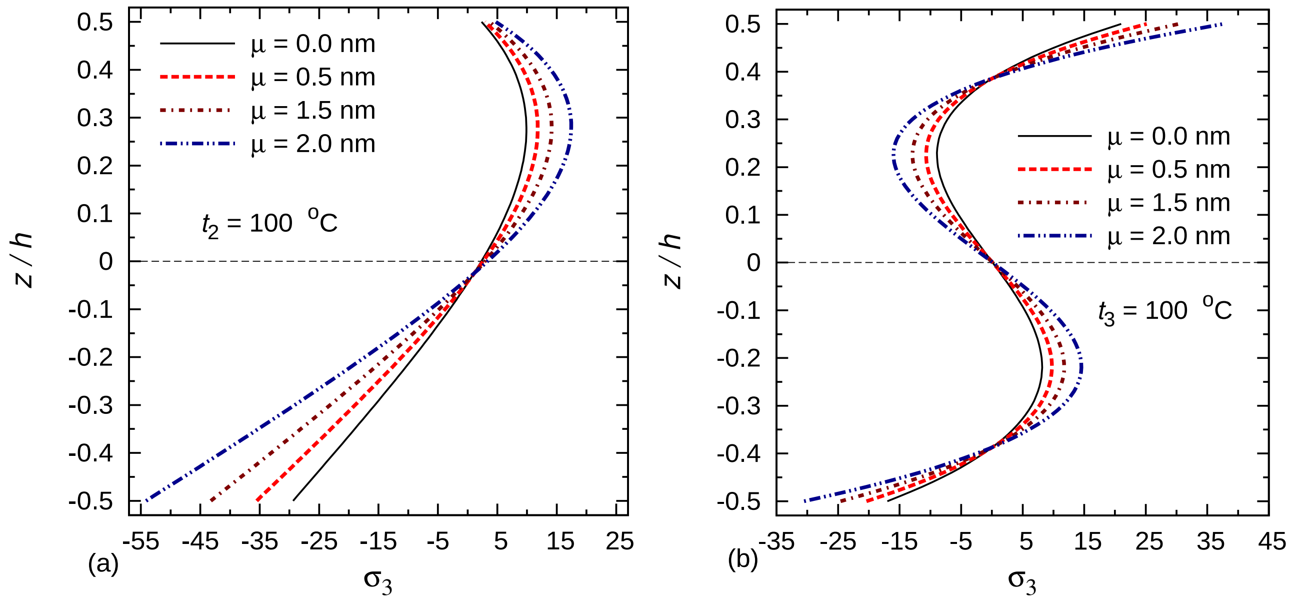

Figure 7. Effect of the nonlocal coefficient μ on the transverse normal stress σ_3 through-the-thickness of FG square nanoplates (**a**) $t_2 = 100, t_3 = 0$ and (**b**) $t_2 = 0, t_3 = 100$ $(a = 10h, \kappa_1 = \kappa_2 = 10)$.

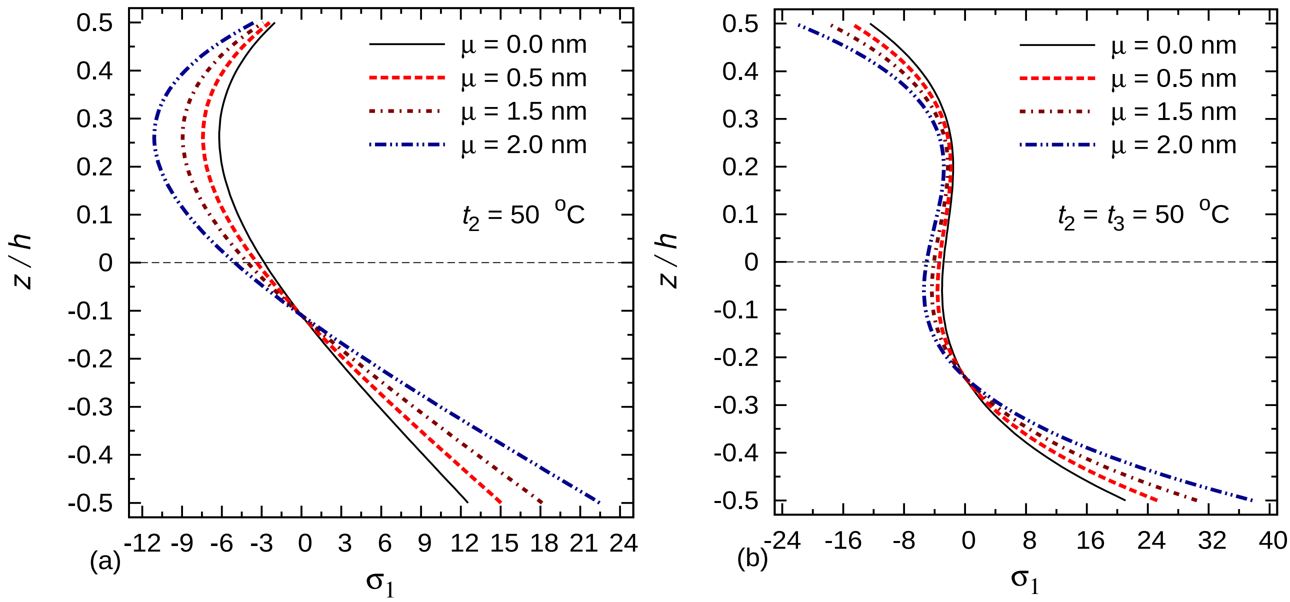

Figure 8. Effect of the nonlocal coefficient μ on the in-plane normal stress σ_1 through-the-thickness of FG square nanoplates (**a**) $t_2 = 50$, $t_3 = 0$ and (**b**) $t_2 = t_3 = 50$ $(a = 10h,\ \kappa_1 = \kappa_2 = 10)$.

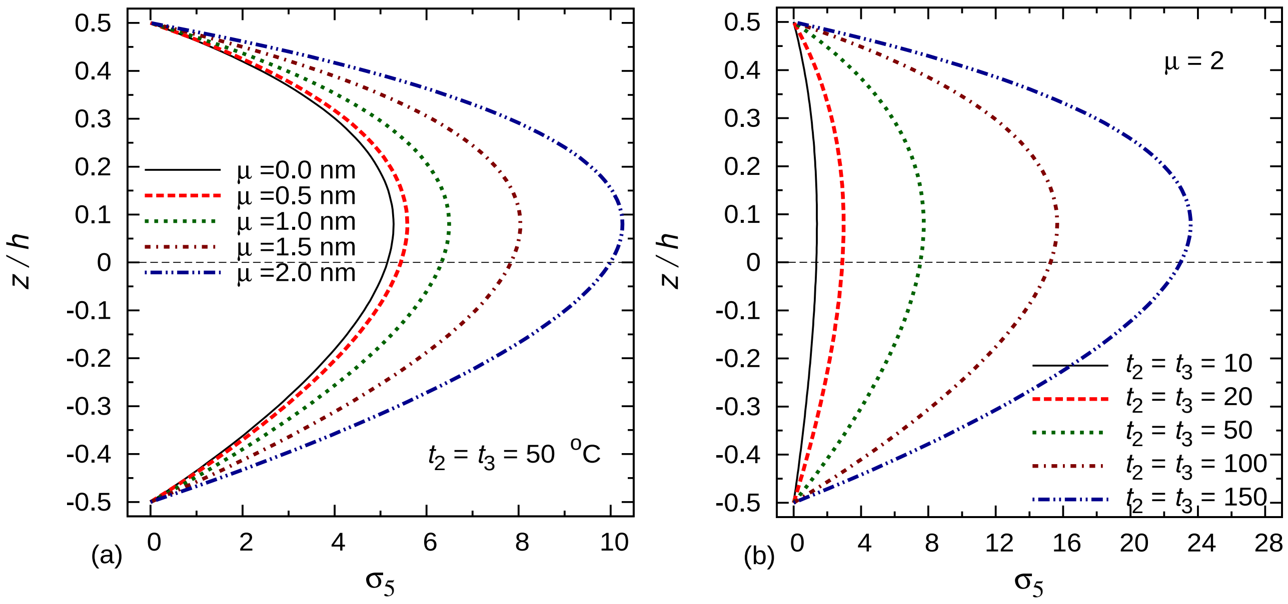

Figure 9. Effects of (**a**) the nonlocal coefficient μ and (**a**) thermal loads t_2 and t_3 on the transverse shear stress σ_5 of FG square nanoplates $(a = 10h, \kappa_1 = \kappa_2 = 10)$.

4.1. Comparison Analyses

To check the reliability and accuracy of the present theory and formulations, five comparison studies were carried out (see Tables 2–6). The first comparison analysis is performed between the in-plane normal stress $\sigma_1(h/3)$ and the deflection $w^*(0)$ in the FG square plates obtained using the proposed theory and those obtained by Carrera et al. [43,44] and Neves et al. [45], as shown in Table 2. The present model gives good results compared to Carrera et al. [43,44] and Neves et al. [45].

Table 3 shows the deflection and stresses are compared to those depicted by Thai and Vo [46]. A good agreement is achieved for all the values of the FG parameter β. As the third example, the deflection $10\bar{w}$ of the square plate under uniformly load is computed and listed in Table 4. The results of the present theories are compared to those presented in Han and Liew [47] and Thai and Choi [26].

The final two comparison analyses (see Tables 5 and 6) are performed between the deflection and stresses obtained by the present theory and the data presented by Sobhy [48] in two cases $(\mu = 0)$ and $(\mu = 2)$ for the FG square nanoplate embedded in elastic foundations for different values β. The local plate is more stiffened than the nonlocal one so the nonlocal theory always over predicts the magnitude of stresses and deflection.

4.2. Benchmark Results

Table 7 shows the effects of the FG parameter β and thermal loads on stresses of a sinusoidally distributed loaded FG plate lying on elastic foundations. It can be seen that the deviation of the deflection caused by the foundation parameter κ_2 is greater than that caused by the spring's parameter κ_1. The deflection is increasing by increasing the thermal parameters t_2 and t_3, but it is decreasing by increasing the parameter β. Table 8 demonstrates the impact of nonlocal parameter μ and thermal loads on the deflection $\bar{w}$ and transverse normal stress σ_3 of a sinusoidally distributed loaded FG square nanoplate embedded in an elastic medium $(\kappa_1 = \kappa_2 = 10, a/h = 10)$. It is established that the deflection $\bar{w}$ and stress σ_3 increase by increasing the nonlocal coefficient μ and the thermal parameters. Due to the increase in thermal parameter t_3 only the transverse normal stress σ_3 decreases.

Effects of (**a**) FG parameter β and (**b**) nonlocal coefficient μ on the deflection $\bar{w}$ through-the-thickness of the FG square nanoplates embedded in an elastic medium $(a = 10h, t_2 = t_3 = 200)$, $(\kappa_1 = \kappa_2 = 10)$, is shown in Figure 3. It is clear that the deflection increases as the nonlocal coefficient μ increases but it is decreasing as the FG parameter β increases. Figure 4 displays the effects of the nonlocal coefficient and thermal loads versus the side-to-thickness ratio a/h on the deflection $\bar{w}$ of the FG square nanoplates embedded in Winkler elastic medium (**a**) $t_2 = t_3 = 0$ and (**b**) $t_2 = t_3 = 50$ $(z/h = 0, \kappa_1 = 10, \kappa_2 = 0)$. The deflection $\bar{w}$ is decreasing with the increase of ratio a/h, and it is rapidly increasing with inclusion of the thermal parameters. Figure 5 shows the effect of the nonlocal coefficient μ on the deflection $\bar{w}$ of the FG nanoplate versus aspect ratio a/b (**a**) $\kappa_1 = \kappa_2 = 0$ and (**b**) $\kappa_1 = \kappa_2 = 10$ $(z/h = 0, a/h = 10, t_2 = t_3 = 50)$. It is clear that the deflection decreases as the parameters κ_1 and κ_2 increase while it increases by increasing the aspect ratio a/b and the nonlocal coefficient μ. Figure 6 shows (**a**) the effect of the nonlocal coefficient μ on the deflection $\bar{w}$ $(z/h = 0)$ and (**b**) effect of the thermal loads t_2 and t_3 on the transverse normal stress σ_3 through the thickness in FG square nanoplates $(\kappa_1 = \kappa_2 = 0,\ a/h = 10)$. The deflection is linearly directly proportional to the thermal load t_2. In addition, the deflection increases as the thermal load t_2 increases; it also increases with the inclusion of the nonlocal coefficient μ. Figure 7 shows the effect of the nonlocal coefficient μ on the transverse normal stress σ_3 through-the-thickness of FG square nanoplates (**a**) $t_2 = 100, t_3 = 0$ and (**b**) $t_2 = 0, t_3 = 100$ $(a = 10h, \kappa_1 = \kappa_2 = 10)$. The tensile stress σ_3 occurs along the upper half-plane, while the compressive stress σ_3 occurs along the lower half-plane of the FG nanoplate. The transverse normal stress σ_3 decreases with the increase of the nonlocal coefficient μ in the lower half-plane while, it increases with the increase of the nonlocal coefficient μ in the upper half-plane in the case of neglecting the thermal parameter t_3. In the case of neglecting the thermal parameter t_2 the maximum value of the transverse normal stress σ_3 occurs at the upper surface of the FG nanoplate. The transverse normal stress σ_3 increases by increasing the nonlocal coefficient μ in the two intervals $0.4 \leq z/h \leq 0.5$ and $-0.4 \leq z/h \leq 0.0$, while it decreases by increasing the nonlocal coefficient μ in the two intervals $0.0 \leq z/h \leq 0.4$ and $-0.5 \leq z/h \leq -0.4$. Figure 8 displays the Effect of the nonlocal coefficient μ on the in-plane normal stress σ_1 through-the-thickness of FG square nanoplates (**a**) $t_2 = 50$, $t_3 = 0$ and (**b**) $t_2 = t_3 = 50$ $(a = 10h,\ \kappa_1 = \kappa_2 = 10)$. The tensile stress σ_1 increases by increasing the nonlocal coefficient μ in the interval $-0.5 \leq z/h \leq -0.1$, while it decreases by increasing the nonlocal coefficient μ in the interval $-0.1 \leq z/h \leq 0.5$, in the case of neglecting the thermal parameter t_3. The tensile stress σ_1 increases by increasing the nonlocal coefficient μ in the interval $-0.5 \leq z/h \leq -0.25$ while it decreases by increasing the nonlocal coefficient μ in the interval $-0.25 \leq z/h \leq 0.5$, in the case of the inclusion of the thermal parameters t_2 and t_3.

Finally, Figure 9 shows the effect of (**a**) the nonlocal coefficient μ and (**b**) thermal loads t_2 and t_3 on the transverse shear stress σ_5 of FG square nanoplates $(a = 10h, \kappa_1 = \kappa_2 = 10)$. It is observed that the shear stress σ_5 increases with the increase in all parameters.

5. Conclusions

A refined plate theory is used for the nonlinear and linear thermal analyses of FG nanoplates resting on an elastic medium under thermal loading using two power-law distributions. The present theory shows a satisfaction of the stress boundary conditions on the upper and lower surfaces of the FG nanoplate by considering both normal and shear deformations by a higher-order variation of all displacements throughout the thickness. The effects of the nonlocal coefficient on the material properties, temperature, and the elastic medium parameters are included in the present numerical results. The effects of several parameters μ, β, a/h, a/b, t_2, t_3, κ_1 and κ_2 are all investigated. The present work shows a good agreement of the results with the ones available in the literature, which demonstrates the accuracy of the results along with the simplicity of the present model in solving the static behavior of the FG nanoplates embedded in an elastic medium in a thermal environment.

Author Contributions: Conceptualization, A.M.Z., M.A.A. and A.F.R.; data curation, A.F.R.; funding acquisition, M.A.A.; investigation, A.M.Z.; methodology, A.M.Z. and A.F.R.; project administration, A.M.Z.; resources, A.F.R.; software, M.A.A. and A.F.R.; supervision, A.M.Z.; validation, A.M.Z.; visualization, A.M.Z.; writing—original draft preparation, M.A.A. and A.F.R.; writing—review and editing, A.M.Z. All authors have read and agreed to the published version of the manuscript.

Funding: The authors extend their appreciation to the Deputyship for Research & Innovation, Ministry of Education in Saudi Arabia for funding this research work through the project number (IFPHI-245-130-2020) and King Abdulaziz University, DSR, Jeddah, Saudi Arabia.

Institutional Review Board Statement: Not applicable.

Informed Consent Statement: Not applicable.

Data Availability Statement: Not applicable.

Acknowledgments: This research work was funded by Institutional Fund Projects under grant no. (IFPHI-245-130-2020). Therefore, authors gratefully acknowledge technical and financial support from the Ministry of Education and King Abdulaziz University, DSR, Jeddah, Saudi Arabia.

Conflicts of Interest: The authors declare no potential conflicts of interest with respect to the research, authorship, and publication of this article.

Appendix A

The elements $\mathcal{D}_{ij}$ and $\mathcal{A}_{ij}$ presented in Equation (11) are given by

$$\{(\mathcal{D}_{11}, \mathcal{D}_{13}, \mathcal{D}_{15}), (\mathcal{D}_{12}, \mathcal{D}_{14}, \mathcal{D}_{16})\} = \int_{-h/2}^{h/2} (1, z, \Psi(z))\{c_{11}, c_{12}\} \mathrm{d}z,$$

$$\{\mathcal{D}_{22}, \mathcal{D}_{24}, \mathcal{D}_{26}\} = \int_{-h/2}^{h/2} c_{22}\{1, z, \Psi(z)\} \mathrm{d}z,$$

$$\{\mathcal{D}_{44}, \mathcal{D}_{45}, \mathcal{D}_{46}\} = \int_{-h/2}^{h/2} z\{zc_{22}, \Psi(z)c_{12}, \Psi(z)c_{22}\} \mathrm{d}z,$$

$$\{(\mathcal{D}_{33}, \mathcal{D}_{35}), (\mathcal{D}_{34}, \mathcal{D}_{36})\} = \int_{-h/2}^{h/2} z(z, \Psi(z))\{c_{11}, c_{12}\} \mathrm{d}z,$$

$$\{\mathcal{D}_{55}, \mathcal{D}_{56}, \mathcal{D}_{66}\} = \int_{-h/2}^{h/2} \Psi^2(z)\{c_{11}, c_{12}, c_{22}\} \mathrm{d}z,$$

$$\mathcal{D}_{17} = \mathcal{D}_{37} = \mathcal{D}_{57} = -\xi \int_{-h/2}^{h/2} c_{13} \Psi^{\backprime\backprime}(z) \mathrm{d}z,$$

$$\mathcal{D}_{27} = \mathcal{D}_{47} = -\xi \int_{-h/2}^{h/2} zc_{23} \Psi^{\backprime\backprime}(z) \mathrm{d}z, \quad \{\mathcal{D}_{23}, \mathcal{D}_{25}\} = \int_{-h/2}^{h/2} c_{12}\{z, \Psi(z)\} \mathrm{d}z,$$

$$\mathcal{D}_{67} = -\xi \int_{-h/2}^{h/2} c_{23} \Psi^{\backprime\backprime} \Psi(z) \mathrm{d}z, \quad \mathcal{D}_{77} = \xi^2 \int_{-h/2}^{h/2} c_{33} (\Psi^{\backprime\backprime})^2 \mathrm{d}z,$$

$$\{\mathcal{A}_{11}, \mathcal{A}_{12}, \mathcal{A}_{13}\} = \int_{-h/2}^{h/2} c_{66}\{1, z, \Psi(z)\} \mathrm{d}z,$$

$$\{\mathcal{A}_{22}, \mathcal{A}_{23}, \mathcal{A}_{33}\} = \int_{-h/2}^{h/2} c_{66}\{z^2, z\Psi(z), \Psi^2(z)\} \mathrm{d}z,$$

$$\{\mathcal{A}_{44}, \mathcal{A}_{55}\} = (\xi + 1)^2 \int_{-h/2}^{h/2} (\Psi^{\backprime\backprime})^2 \{c_{55}, c_{44}\} \mathrm{d}z.$$

Appendix B

The elements $\mathcal{K}_{ij} = \mathcal{K}_{ji}$ presented in Equation (14) are given by

$$
\begin{aligned}
\mathcal{K}_{11} =&\mathcal{D}_{11}\partial^2_{xx} + \mathcal{A}_{11}\partial^2_{yy},\\
\mathcal{K}_{12} =&(\mathcal{D}_{12} + \mathcal{A}_{11})\partial^2 yx,\\
\mathcal{K}_{13} =&\Big[-\mathcal{D}_{15}\partial^2_{xx} - (\mathcal{D}_{14} + 2\mathcal{A}_{12})\partial^2_{yy}\Big]\partial_x,\\
\mathcal{K}_{14} =&\Big[\mathcal{D}_{17} - \mathcal{D}_{15}\partial^2_{xx} - (\mathcal{D}_{16} + 2\mathcal{A}_{13})\partial^2_{yy}\Big]\partial_x,\\
\mathcal{K}_{22} =&\mathcal{A}_{11}\partial^2_{xx} + \mathcal{D}_{22}\partial^2_{yy},\\
\mathcal{K}_{23} =&\Big[-\mathcal{D}_{24}\partial^2_{yy} - (\mathcal{D}_{23} + 2\mathcal{A}_{12})\partial^2_{xx}\Big]\partial_y,\\
\mathcal{K}_{24} =&\Big[\mathcal{D}_{27} - \mathcal{D}_{26}\partial^2_{yy} - (\mathcal{D}_{25} + 2\mathcal{A}_{13})\partial^2_{xx}\Big]\partial_y,\\
\mathcal{K}_{33} =&\Big[\mathcal{D}_{33}\partial^2_{xx} + 2(\mathcal{D}_{34} + 2\mathcal{A}_{22})\partial^2_{yy} - K_2\Re\Big]\partial^2_{xx} + \Big[\mathcal{D}_{44}\partial^2_{yy} - K_2\Re\Big]\partial^2_{yy} + K_1\Re,\\
\mathcal{K}_{34} =&\Big[\mathcal{D}_{35}\partial^2_{xx} + 2(\mathcal{D}_{36} + 2\mathcal{A}_{23})\partial^2_{yy} - \mathcal{D}_{37} - K_2\Re\Big]\partial^2_{xx} +\\
&\Big[\mathcal{D}_{46}\partial^2_{yy} - \mathcal{D}_{47} - K_2\Re\Big]\partial^2_{yy} + K_1\Re,\\
\mathcal{K}_{44} =&\Big[\mathcal{D}_{55}\partial^2_{xx} + 2(\mathcal{D}_{56} + 2\mathcal{A}_{33})\partial^2_{yy} - (\mathcal{A}_{44} + 2\mathcal{D}_{57}) - K_2\Re\Big]\partial^2_{xx} +\\
&\Big[\mathcal{D}_{66}\partial^2_{yy} - (\mathcal{A}_{55} + 2\mathcal{D}_{67}) - K_2\Re\Big]\partial^2_{yy} + K_1\Re + \mathcal{D}_{77},
\end{aligned}
$$

Appendix C

The elements $\mathcal{H}_{ij} = \mathcal{H}_{ji}$ presented in Equation (19) are given by

$$
\begin{aligned}
\mathcal{H}_{11} =& -\mathcal{D}_{11}\lambda_m^2 - \mathcal{A}_{11}\gamma_n^2,\\
\mathcal{H}_{12} =& -\lambda_m\gamma_n(\mathcal{D}_{12} + \mathcal{A}_{11}),\\
\mathcal{H}_{13} =&\lambda_m\Big[\lambda_m^2\mathcal{D}_{13} + \gamma_n^2(\mathcal{D}_{14} + 2\mathcal{A}_{12})\Big],\\
\mathcal{H}_{14} =&\lambda_m\Big[\lambda_m^2\mathcal{D}_{15} + \gamma_n^2(\mathcal{D}_{16} + 2\mathcal{A}_{13}) + \mathcal{D}_{17}\Big],\\
\mathcal{H}_{22} =& -\lambda_m^2\mathcal{A}_{11} - \gamma_n^2\mathcal{D}_{22},\\
\mathcal{H}_{23} =&\gamma_n\Big[\gamma_n^2\mathcal{D}_{24} + \lambda_m^2(\mathcal{D}_{23} + 2\mathcal{A}_{12})\Big],\\
\mathcal{H}_{24} =&\gamma_n\Big[\gamma_n^2\mathcal{D}_{26} + \lambda_m^2(\mathcal{D}_{25} + 2\mathcal{A}_{13}) + \mathcal{D}_{27}\Big],\\
\mathcal{H}_{33} =& -\gamma_n^2\Big[K_2\Big(1 + \mu^2\Big(\lambda_m^2 + \gamma_n^2\Big)\Big) + \mathcal{D}_{44}\gamma_n^2 + 2\lambda_m^2(\mathcal{D}_{34} + 2\mathcal{A}_{22})\Big]\\
&-\lambda_m^2\Big(\mathcal{D}_{33}\lambda_m^2 + K_2\Big(1 + \mu^2\Big(\lambda_m^2 + \gamma_n^2\Big)\Big)\Big) - K_1\Big(1 + \mu^2\Big(\lambda_m^2 + \gamma_n^2\Big)\Big),\\
\mathcal{H}_{34} =& -\gamma_n^2\Big[K_2\Big(1 + \mu^2\Big(\lambda_m^2 + \gamma_n^2\Big)\Big) + \mathcal{D}_{47} + \mathcal{D}_{46}\gamma_n^2 + \lambda_m^2(\mathcal{D}_{36} + \mathcal{D}_{45} + 4\mathcal{A}_{23})\Big]\\
&-\lambda_m^2\Big(\mathcal{D}_{33}\lambda_m^2 + \mathcal{D}_{37} + K_2\Big(1 + \mu^2\Big(\lambda_m^2 + \gamma_n^2\Big)\Big)\Big) - K_1\Big(1 + \mu^2\Big(\lambda_m^2 + \gamma_n^2\Big)\Big),
\end{aligned}
$$

$$
\begin{aligned}
\mathcal{H}_{44} =& -\lambda_m^2\Big[K_2\Big(1 + \mu^2\Big(\lambda_m^2 + \gamma_n^2\Big)\Big) + \mathcal{A}_{44} + 2\mathcal{D}_{75} + \mathcal{D}_{55}\lambda_m^2 + 2\gamma_n^2(\mathcal{D}_{56} + 2\mathcal{A}_{33})\Big]\\
&-\gamma_n^2\Big[K_2\Big(1 + \mu^2\Big(\lambda_m^2 + \gamma_n^2\Big)\Big) + \mathcal{D}_{66}\gamma_n^2 + \mathcal{A}_{55} + 2\mathcal{D}_{67}\Big]\\
&-K_1\Big(1 + \mu^2\Big(\lambda_m^2 + \gamma_n^2\Big)\Big).
\end{aligned}
$$

The elements $e_{ij}^{\mathcal{T}}$ presented in Equation (21) are given by

$$
\begin{aligned}
\{e^T_{11}, e^T_{12}, e^T_{13}\} &= \frac{1}{h}\int_{-h/2}^{h/2} (c_{11}+c_{12}+c_{13})\{h, z, \Psi(z)\}\alpha(z)\mathrm{d}z,\\
\{e^T_{21}, e^T_{22}, e^T_{23}\} &= \frac{1}{h}\int_{-h/2}^{h/2} (c_{12}+c_{22}+c_{23})\{h, z, \Psi(z)\}\alpha(z)\mathrm{d}z,\\
\{e^T_{31}, e^T_{32}, e^T_{33}\} &= \frac{1}{h}\int_{-h/2}^{h/2} z(c_{11}+c_{12}+c_{13})\{h, z, \Psi(z)\}\alpha(z)\mathrm{d}z,\\
\{e^T_{41}, e^T_{42}, e^T_{43}\} &= \frac{1}{h}\int_{-h/2}^{h/2} z(c_{12}+c_{22}+c_{23})\{h, z, \Psi(z)\}\alpha(z)\mathrm{d}z,\\
\{e^T_{51}, e^T_{52}, e^T_{53}\} &= \frac{1}{h}\int_{-h/2}^{h/2} \Psi(z)(c_{11}+c_{12}+c_{13})\{h, z, \Psi(z)\}\alpha(z)\mathrm{d}z,\\
\{e^T_{61}, e^T_{62}, e^T_{63}\} &= \frac{1}{h}\int_{-h/2}^{h/2} \Psi(z)(c_{12}+c_{22}+c_{23})\{h, z, \Psi(z)\}\alpha(z)\mathrm{d}z,\\
\{e^T_{71}, e^T_{72}, e^T_{73}\} &= -\frac{\xi}{h}\int_{-h/2}^{h/2} \Psi''(c_{13}+c_{23}+c_{33})\{h, z, \Psi(z)\}\alpha(z)\mathrm{d}z.
\end{aligned}
$$

References

1. Aifantis, E.C. Strain gradient interpretation of size effects. *Int. J. Fract.* **1999**, *95*, 299–314. [CrossRef]
2. Reddy, J.N. Nonlocal theories for bending, buckling and vibration of beams. *Int. J. Eng. Sci.* **2007**, *45*, 288–307. [CrossRef]
3. Hashemi, S.H.; Samaei, A.T. Buckling analysis of micro/nanoscale plates via nonlocal elasticity theory. *Physica E* **2011**, *43*, 1400–1404. [CrossRef]
4. Zenkour, A.M.; Sobhy, M. Nonlocal elasticity theory for thermal buckling of nanoplates lying on Winkler-Pasternak elastic substrate medium. *Physica E* **2013**, *53*, 251–259. [CrossRef]
5. Sobhy, M. Thermomechanical bending and free vibration of single-layered graphene sheets embedded in an elastic medium. *Physica E* **2014**, *56*, 400–409. [CrossRef]
6. Yang, B.; Ding, H.J.; Chen, W.Q. Elasticity solutions for functionally graded rectangular plates with two opposite edges simply-supported. *Appl. Math. Model.* **2012**, *36*, 488–503. [CrossRef]
7. Birman, V.; Byrd, L.W. Modeling and analysis of functionally graded materials and structures. *Appl. Mech. Rev.* **2007**, *60*, 195–216. [CrossRef]
8. Mantari, J.L.; Guedes Soares, C. A novel higher-order shear deformation theory with stretching effect for functionally graded plates. *Compos. Part B Eng.* **2013**, *45*, 268–2681. [CrossRef]
9. Wang, Z.X.; Shen, H.-S. Nonlinear dynamic response of sandwich plates with FGM face sheets resting on elastic foundations in thermal environments. *Ocean Eng.* **2013**, *57*, 99–110. [CrossRef]
10. Sofiyev, A.H. Thermal buckling of FGM shells resting on a two parameter elastic foundation. *Thin-Walled Struct.* **2011**, *49*, 1304–1311. [CrossRef]
11. Duc, N.D.; Tung, H.V. Mechanical and thermal postbuckling of higher-order shear deformable functionally graded plates on elastic foundations. *Compos. Struct.* **2011**, *93*, 2874–2881. [CrossRef]
12. Kasaeian, A.B.; Vatan, S.N.; Daneshmand, S. FGM materials and finding an appropriate model for the thermal conductivity. *Procedia Eng.* **2011**, *14*, 3199–3204. [CrossRef]
13. Sepahi, O.; Forouzan, M.R.; Malekzadeh, P. Large deflection analysis of thermo-mechanical loaded annular FGM plates on nonlinear elastic foundation via DQM. *Compos. Struct.* **2010**, *92*, 2369–2378. [CrossRef]
14. Hashemi, S.H.; Bedroud, M.; Nazemnezhad, R. An exact analytical solution for free vibration of functionally graded circular/annular Mindlin nanoplates via nonlocal elasticity. *Compos. Struct.* **2013**, *103*, 108–118. [CrossRef]
15. Nazemnezhad, R.; Hashemi, S.H. Nonlocal nonlinear free vibration of functionally graded nanobeams. *Compos. Struct.* **2014**, *110*, 192–199. [CrossRef]
16. Hashemi, S.H.; Nazemnezhad, R.; Bedroud, M. Surface effects on nonlinear free vibration of functionally graded nanobeams using nonlocal elasticity. *Appl. Math. Model.* **2014**, *38*, 3538–3553. [CrossRef]
17. Hashemi, S.H.; Nahas, I.; Fakher, M.; Nazemnezhad, R. Surface effects on free vibration of piezoelectric functionally graded nanobeams using nonlocal elasticity. *Acta Mech.* **2014**, *225*, 1555–1564. [CrossRef]
18. Thai, H.T.; Vo, T.P. A nonlocal sinusoidal shear deformation beam theory with application to bending, buckling, and vibration of nanobeams. *Int. J. Eng. Sci.* **2012**, *54*, 58–66. [CrossRef]
19. Eringen, A.C.; Edelen, D.G.B. On nonlocal elasticity. *Int. J. Eng. Sci.* **1972**, *10*, 233–248. [CrossRef]
20. Zenkour, A.M.; Allam, M.N.M.; Radwan, A.F. Bending of cross-ply laminated plates resting on elastic foundations under thermo-mechanical loading. *Int. J. Mech. Mater. Des.* **2013**, *9*, 239–251. [CrossRef]
21. Zenkour, A.M.; Allam, M.N.M.; Radwan, A.F. Effects of hygrothermal conditions on cross-ply laminated plates resting on elastic foundations. *Arch. Civ. Mech. Eng.* **2014**, *14*, 144–159. [CrossRef]
22. Winkler, E. *Die Lehre von der Elastizität and Festigkeit*; Dominicus: Prague, Czech Republic, 1867.

23. Zenkour, A.M.; Allam, M.N.M.; Shaker, M.O.; Radwan, A.F. On the simple and mixed first-order theories for plates resting on elastic foundations. *Acta Mech.* **2011**, *220*, 33–46. [CrossRef]
24. Zenkour, A.M.; Radwan, A.F. On the simple and mixed first-order theories for functionally graded plates resting on elastic foundations. *Meccanica* **2013**, *48*, 1501–1516. [CrossRef]
25. Thai, H.-T.; Choi, D-H. A refined plate theory for functionally graded plates resting on elastic foundation. *Compos. Sci. Technol.* **2011**, *71*, 1850–1858. [CrossRef]
26. Thai, H.-T.; Choi, D-H. A simple refined theory for bending, buckling, and vibration of thick plates resting on elastic foundation. *Int. J. Mech. Sci.* **2013**, *73*, 40–52. [CrossRef]
27. Yas, M.H.; Tahouneh, V. 3-D Free vibration analysis of thick functionally graded annular plates on Pasternak elastic foundation via differential quadrature method (DQM). *Acta Mech.* **2012**, *223*, 43–62. [CrossRef]
28. Shen, H.-S. Nonlinear analysis of simply-supported Reissner-Mindlin plates subjected to lateral pressure and thermal loading and resting on two-parameter elastic foundations. *Eng. Struct.* **2000**, *23*, 1481–1493. [CrossRef]
29. Zenkour, A.M. Thermo-electrical buckling response of actuated functionally graded piezoelectric nanoscale plates. *Results Phys*. **2019**, *13*, 102192. [CrossRef]
30. Alzahrani, E.O.; Zenkour, A.M.; Sobhy, M. Small scale effect on hygro-thermomechanical bending of nanoplates embedded in an elastic medium. *Compos. Struct*. **2013**, *105*, 163–172. [CrossRef]
31. Zenkour, A.M.; Sobhy, M. Nonlocal piezo-hygrothermal analysis for vibration characteristics of a piezoelectric Kelvin-Voigt viscoelastic nanoplate embedded in a viscoelastic medium. *Acta Mech*. **2018**, *229*, 3–19. [CrossRef]
32. Zenkour, A.M. Bending of FGM plates by a simplified four-unknown shear and normal deformations theory. *Int. J. Appl. Mech.* **2013**, *5*, 1350020. [CrossRef]
33. Zenkour, A.M. A simple four-unknown refined theory for bending analysis of functionally graded plates. *Appl. Math. Model.* **2013**, *37*, 9041–9051. [CrossRef]
34. Zenkour, A.M. Bending analysis of functionally graded sandwich plates using a simple four-unknown shear and normal deformations theory. *J. Sandw. Struct. Mater.* **2013**, *15*, 629–656. [CrossRef]
35. Al Khateeb, S.A.; Zenkour, A.M. A refined four-unknown plate theory for advanced plates resting on elastic foundations in hygrothermal environment. *Compos. Struct.* **2014**, *111*, 240–248. [CrossRef]
36. Zenkour, A.M. Thermal bending of layered composite plates resting on elastic foundations using four-unkown shear and normal deformations theory. *Compos. Struct.* **2015**, *122*, 260–270. [CrossRef]
37. Zenkour, A.M. A simplified four-unknown shear and normal deformations theory for bidirectional laminated plates. *Sadhana Acad. Proc. Eng. Sci.* **2015**, *40*, 215–234. [CrossRef]
38. Thai, C.H.; Zenkour, A.M.; Abdel Wahab, M.; Thai, H.N. A simple four-unknown shear and normal deformations theory for functionally graded isotropic and sandwich plates based on isogeometric analysis. *Compos. Struct.* **2016**, *139*, 77–95. [CrossRef]
39. Eringen, A.C. On differential-equations of nonlocal elasticity and solutions of screw dislocation and surface-waves. *J. Appl. Phys.* **1983**, *54*, 4703–4710. [CrossRef]
40. Eringen, A.C. *Nonlocal Continuum Field Theories*; Springer: New York, NY, USA, 2002.
41. Eringen, A.C. Theory of micropolar plates. *Z. Angew. Math. Phys.* **1967**, *18*, 12–30. [CrossRef]
42. Eringen, A.C. Nonlocal polar elastic continua. *Int. J. Eng. Sci.* **1972**, *10*, 1–16. [CrossRef]
43. Carrera, E.; Brischetto, S.; Cinefra, M.; Soave, M. Effects of thickness stretching in functionally graded plates and shells. *Compos. Part B* **2011**, *42*, 123–133. [CrossRef]
44. Carrera, E.; Brischetto, S.; Robaldo, A. Variable kinematic model for the analysis of functionally graded material plates. *AIAA J.* **2008**, *46*, 194–203. [CrossRef]
45. Neves, A.M.A.; Ferreira, A.J.M.; Carrera, E.; Roque, C.M.C.; Cinefra, M.; Jorge, R.M.N.; Soares, C.M.M. Bending of FGM plates by a sinusoidal plate formulation and collocation with radial basis functions. *Mech. Res. Commun.* **2011**, *38*, 368–371. [CrossRef]
46. Thai, H.-T.; Vo, T.P. A new sinusoidal shear deformation theory for bending, buckling, and vibration of functionally graded plates. *Appl. Math. Model.* **2013**, *37*, 3269–3281. [CrossRef]
47. Han, J.B.; Liew, K.M. Numerical differential quadrature method for Reissner/Mindlin plates on two-parameter foundations. *Int. J. Mech. Sci.* **1997**, *39*, 977–989. [CrossRef]
48. Sobhy, M. A comprehensive study on FGM nanoplates embedded in an elastic medium. *Compos. Struct.* **2015**, *134*, 966–980. [CrossRef]